Journal of Solid State Chemistry **149,** 16–20 (2000)
Article ID jssc.1999.8474, available online at http://www.idealibrary.com on IDEAL®

Phase Transformations in Gel-Derived and Mixed-Powder-Derived Yttrium Disilicate, $Y_2Si_2O_7$, by X-Ray Diffraction and ^{29}Si MAS NMR

Julien Parmentier,* Philippe R. Bodart,† Ludovic Audoin,‡ Georges Massouras,§ Derek P. Thompson,* Robin K. Harris,† Paul Goursat,‡ and Jean-Louis Besson§

*Department of Mechanical, Materials and Manufacturing Engineering, University of Newcastle, Newcastle upon Tyne, NE1 7RU, United Kingdom; †Department of Chemistry, University of Durham, South Road, Durham, DH1 3LE United Kingdom; ‡Faculté des Sciences, Laboratoire des Matériaux Céramiques et Traitements des Surfaces, UPRESA 6015, 123 Avenue Albert Thomas, 87060 Limoges Cedex, France; and §Laboratoire des Matériaux Céramiques et Traitements des Surfaces, UPRESA 6015, Ecole Nationale Supérieure des Céramiques Industrielles, 47 Avenue Albert Thomas, 87065 Limoges Cedex, France

Received December 7, 1998; in revised form August 3, 1999; accepted August 10, 1999

The different polymorphs of $Y_2Si_2O_7$ have been synthesized by a sol–gel process and by mixed-powder routes. Their ranges of stability are discussed as a function of heat-treatment and synthesis route. It appeared that amorphous sol–gel samples crystallized according to the sequence amorphous $\rightarrow \alpha \rightarrow \beta \rightarrow \gamma$, even when isothermal heat-treatments were performed, regardless of temperature. It is proposed that preferential crystallization of α is related to the type of silicon structural units in the starting amorphous precursor similar to α phase. High-resolution ^{29}Si NMR spectra (linewidth $\leq$ 21 Hz) are reported for the α, β, γ, and δ, polymorphs which are consistent with accepted structural data from the point of view of the number of sites, the populations, and the relative chemical shifts. © 2000 Academic Press

1. INTRODUCTION

The binary disilicates, and especially the rare earth disilicates $(RE)_2Si_2O_7$, have been widely studied for their unique magnetic, electrical, and optical properties (1). They are also well known for their polymorphism, exhibiting up to seven different structure types (at normal pressure), depending on the temperature and the nature of the rare earth cation (1, 2). Yttrium disilicate, $Y_2Si_2O_7$, shows five (or possibly six) structural forms (y, α, β, γ, δ, and z). One of them, the yttriallite low form (3), also called y (4), is only stable up to 1200°C and can contain "stabilizing impurities" such as H^+, Na^+, Mg^{2+}, Mn^{2+}, Fe^{2+}, Fe^{3+}, Al^{3+}, Th^{4+}, or Zr^{4+} (2). Recent studies by Liddell and Thompson (5) have shown that, in the Y–Si–Al–O–N system, this phase can be obtained up to 1400°C. This increase in the thermal stability could be due to the stabilization of the y-structure by impurities such as Al^{3+} and/or N^{3-}. The four other phases, α, β, γ, and δ (also called B, C, D, and E types, respectively (1)) were classified by Ito and Johnson according to their increasing stability with temperature, following the sequence (2)

$$\alpha \xrightleftharpoons{1225^\circ C} \beta \xrightleftharpoons{1445^\circ C} \gamma \xrightleftharpoons{1535^\circ C} \delta.$$

Their structures, usually determined for members of the isostructural rare-earth compounds, are generally built up of $[Si_2O_7]^{6-}$ units linked by cations (y, β, γ, δ) or, for the α-structure, of $[Si_3O_{10}]^{8-}$ groups plus additional $[SiO_4]^{4-}$ tetrahedra. X-ray diffraction of a single crystal of α-$Ho_2Si_2O_7$ has shown four silicon environments and Si–O–Si bond angles of 118.2° and 133.2° (1). For y-$(Th, Y)_2Si_2O_7$, the same technique has shown two silicon sites and a bond angle of 134° (4). The δ-$Y_2Si_2O_7$ phase exhibits two sites and a bond angle of 158° (1, 6, 7). For β and γ, a single silicon site is observed for rare-earth and yttrium disilicates, respectively, and space-group considerations predict a bond angle of 180° (1, 6). Interestingly, a recent study has reported a value of 172° for the γ-$Y_2Si_2O_7$ phase (7). Another form, z-$Y_2Si_2O_7$, has been reported only once (2) (JCPDS card 21-1459), with an unindexed powder diffraction pattern. This phase seems to be a low-temperature form, stable only below 1030°C.

More recently, the use of Y_2O_3 (8) (and to a lesser extent rare earth oxides (9, 10) as sintering additives for silicon nitride and in the formulation of new oxynitride M–Si–Al–O–N phases (M = Y, Ln) (11) has generated a revival of interest in phase transformations in the $Y_2Si_2O_7$ system. Some of its forms appear in Si_3N_4 grain boundaries, often as a secondary phase in the synthesis of M–Si–Al–O–N compounds, either in the as-prepared state or after oxidation (12). Differences in the polymorph stability ranges were noticed (13, 14) compared to the sequence given by Ito and Johnson previously. This could be due to the origin of the sample (pure oxide, nitride synthesis, nitride oxidation product) and/or the presence of impurities (Al, Fe,

0022-4596/00 $35.00

Ti, N) stabilizing one polymorph relative to another. The present study explored the influence of the synthesis route on the product in the Y–Si–O system. Two routes were explored, namely, sol–gel (SG) and mixed-powder (MP), chosen because of their difference in reactivity. Moreover, the absence in the literature of resolved ^{29}Si MAS NMR spectra for all the yttrium disilicate forms provided the driving force for our study of these phases by NMR.

2. EXPERIMENTAL

Synthesis

The mixed-powder (MP) route involved mixing Y_2O_3 (H.C. Starck, grade A) and SiO_2 (BDH, 99.9%) in stoichiometric amounts in isopropanol in an agate mortar. The dried powder was then pressed into a pellet and sintered in nitrogen at 1700°C for 2 h. The densified pellet was subsequently heat-treated at lower temperatures.

The sol–gel (SG) route used for these studies was derived from the synthesis described by Hulling and Messing (15) for the production of a well-homogenized gel in the Al_2O_3–SiO_2 system and is not repeated here. The aluminum salt ($Al(NO_3)_3 \cdot 9H_2O$) was replaced by yttrium nitrate, $Y(NO_3)_3 \cdot 5H_2O$ (Aldrich, 99.9%), and the silicon was introduced via TetraEthylOrthoSilicate, TEOS (Aldrich, 99%). The hydrolysis reaction was performed only by the water of crystallization in the yttrium nitrate leading to a very long gelation time ($\approx$ 3 weeks), which also proved to contribute to a good homogeneity (16). The final concentration of the TEOS and Y^{3+} in the gel was 0.5 M. The gel was dried at 80°C and calcined at 600°C before being given further heat-treatment at higher temperatures.

Characterization

X-ray diffraction (XRD) studies were carried out using a Hägg–Guinier focusing camera and Cu$K\alpha_1$ radiation. KCl was used as an internal standard. Differential Thermal Analysis (DTA) was performed on the SG sample previously calcined at 600°C using a Stanton Redcroft DTA674 instrument in air at a heating rate of 10°C/min. Silicon-29 MAS NMR spectra were obtained with a Varian 300 Unity-plus spectrometer operating at a frequency of 59.6 MHz. The samples were packed in zirconia rotors and spun at 3–4 kHz. Chemical shifts are reported relative to the signal for tetramethylsilane. No line-broadening was applied prior to Fourier transformation.

3. RESULTS AND DISCUSSION

X-Ray Diffraction

The phases detected on the XRD patterns for the samples heat-treated at different temperatures are reported in Tables 1 and 2 for MP and SG routes, respectively.

TABLE 1
Heat-Treatments Carried Out on the MP Samples and the Corresponding Crystalline Phases Detected by XRD

	Heat treatment		
	Temperature (°C)	Time (hours)	Crystalline phases
Initial treatment	1700	2	δ (s), Ap (mw)
Subsequent treatment	1400	6	γ (s), Ap (mw), β (traces)
	1200	16	β (s), Ap (mw), δ (w)

Note. (s) strong; (m) medium; (w) weak; Ap, apatite $Y_{4.67}(SiO_4)_3O$; β, γ, δ, polymorphs of $Y_2Si_2O_7$.

MP route. For the MP sample calcined at 1700°C, δ-$Y_2Si_2O_7$ (JCPDS card 42-168) and oxy-apatite, $Y_{4.67}(SiO_4)_3O$ (JCPDS card 30-1457), were detected, in agreement with the literature (2, 17), in which these phases are reported as being stable above 1535 and 1650°C, respectively. Nevertheless, the presence of a yttrium-rich, apatite phase in addition to $Y_2Si_2O_7$, indicates incomplete reaction, and this should react further with amorphous silica to give a $Y_2Si_2O_7$ overall product. Subsequent heat treatment at lower temperatures allowed the solid–solid transformation $\delta \rightarrow \gamma$ or $\delta \rightarrow \beta$ to take place but at a slow rate as shown by the systematic presence of two forms even after long calcination times. The transition $\delta \rightarrow \alpha$ was not observed even at 1200°C, although this is in the reported range of

TABLE 2
Heat-Treatments Carried Out on SG Samples and the Corresponding Crystalline Phases Detected by XRD

Heat treatment		
Temperature (°C)	Time	Crystalline phases
600	2 h	amorphous
840	3 days	α (s), y (m)
900	24 h	y(s), Ap (w), α (w)
975	46 h Q	α (s), Ap (w)
1060	3 min	α (s), X2 Y_2SiO_5 (m), Ap (m)
1150	24 h Q	α (s), Apatite (w)
1200	24 h I, Q	α (s), Ap (traces)
1300	24 h I, Q	α (s), β (m), Ap (traces)
1350	24 h I, Q	β (s), γ (w), X2 Y_2SiO_5 (traces)
1350	3 min I, Q	α (s), X2 Y_2SiO_5 (mw), β (mw), Y_2O_3 (mw)
1400	24 h I	β (s), γ (m)
1500	3 min I, Q	α (s), β (m), X2 Y_2SiO_5 (mw), Y_2O_3 (mw)
1500	2 h I, Q	β (s), Y_2O_3 (traces)
1600	2 h I, Q	γ (s), β (s), Y_2O_3 (traces)

Note. I, isothermal calcination; Q, quench in air; (s) strong; (m) medium; (w) weak; Ap, apatite $Y_{4.67}(SiO_4)_3O$); y, α, β, γ, δ, polymorphs of $Y_2Si_2O_7$.

thermal stability of α. It is worth noting that, in rare-earth disilicate systems, the transformation from high-temperature to low-temperature forms proceeds by a solid state mechanism with a large time constant. For $Eu_2Si_2O_7$ (which shows only α and δ forms), the transformation $\delta \rightarrow \alpha$ has never been observed within a reasonable period of time (i.e., 100 h). This fact suggested to Flesch (1) that the $\delta \rightarrow \alpha$ transition is reconstructive, which is well understood in the light of the given structural information. The $\delta \rightarrow \alpha$ transformation results in the breaking of the Si–O–Si bonds (of the double-tetrahedra groups) in the δ structure to achieve the (Si_3O_{10}) configuration in the α-structure; i.e.,

$$2(Si_2O_7^{6-}) \leftrightarrows (Si_3O_{10}^{8-}) + SiO_4^{4-}.$$

Nevertheless, the general trend of stability for the different structural forms as a function of temperature is verified even if the ranges of temperature are slightly modified from those in the literature.

SG route. For the sol–gel route, the xerogel is still amorphous after calcination at 600°C. DTA subsequently performed on such a sample showed an exothermic peak at 1060°C which was attributed to the crystallization of α-phase. Treatments below this temperature yielded y or α according to the calcination time. The y form (usually only obtained in the presence of impurities) is possibly stabilized by residual hydroxyl groups present at this temperature. A longer heat-treatment time promotes the formation of α by removing these hydroxyl groups. The poor crystallinity of y-$Y_2Si_2O_7$ is related to the low preparation temperature and the presence of additional unindexed peaks which did not allow complete characterization of the X-ray pattern and a distinction to be made between the different indexings given in the literature for "pure" y-$Y_2Si_2O_7$ (monoclinic $P2_1/m$ (18) or orthorhombic *Aba*2 (19)).

The α form was the main phase observed at 1200°C in agreement with the literature (2). At higher temperatures and for short isothermal heat-treatments (3 min), α was always the major phase detected, indicating a preferential crystallization from the amorphous state even at temperatures outside its range of thermal stability. Longer calcinations (24 h) were necessary to obtain the transformation of α to the higher temperature forms in relation to the low rate of reconstruction of the crystalline structure. Moreover, the phase transformation seems to follow the sequence $\alpha \rightarrow \beta \rightarrow \gamma$ and not directly $\alpha \rightarrow \gamma$ as depicted in Table 2 for temperatures in between 1400 and 1600°C. The successive nature of the transformation sequence and the slow kinetics probably explain why the δ-form was never observed even at temperatures as high as 1600°C. This phase formed more easily by solid state reaction between Y_2O_3 and SiO_2 at 1700°C rather than by a polymorphic transformation; this fact could be related to the higher free energy decrease in the former case. The range of thermal stability for γ seems to be different from that previously reported in the literature; actually it appeared on calcination at 1350°C instead of at 1450°C.

Form β appeared at 1300°C and was always present after quenching from higher temperatures (1600°C). Form γ was always present above 1350°C (instead of 1535°C) and was always associated with β.

Silicon-29 MAS NMR

Silicon-29 MAS NMR spectra were obtained for the xerogel during its thermal evolution and for the different structural forms of $Y_2Si_2O_7$ (y, α, β, γ, δ).

The spectrum of the gel dried at 80°C exhibits a broad peak (characteristic of an amorphous phase) at −102 ppm with a shoulder at −110 ppm (Fig. 1a). These chemical shifts, typical of highly condensed silica species (Q^4 and Q^3), may be assigned to O_4Si and O_3Si–OH (or O_3–Si–O^-Y^{3+}), consistent with the formation of a three-dimensional network in the gel.

After calcination at 600°C, a broad peak is observed at approximately −80 ppm (Fig. 1b). Its deconvolution led to three peaks with chemical shifts of −81.4, −89.2, −96.0 ppm in corresponding intensities of 5, 1, and 1, respectively. This is related mainly to the presence of Q^1 and Q^2 species. This lower condensation of the silica species is a result of the cleaving of some Si–O–Si bonds, due to the incorporation of Y_2O_3 into the silica network. These spectra show that, even at low temperatures (600°C), structural rearrangements take place in the amorphous state, yielding a local silicate environment probably similar to those in the low-temperature forms y and α (i.e., [$Si_2O_7^{6-}$]

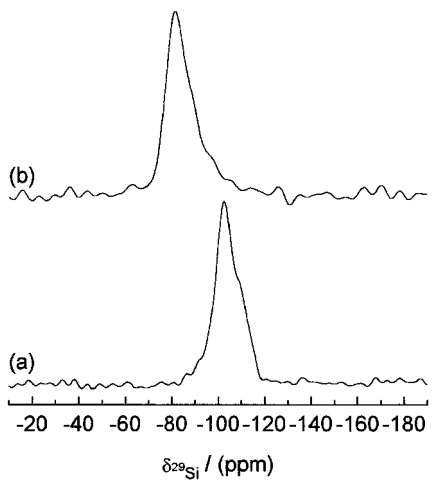

FIG. 1. Silicon-29 spectra of (a) the gel dried at 80°C, obtained by ^1H cross-polarisation (4 ms contact-time); 1056 transients were recorded with a recycle delay of 2 s. (b) The gel calcined at 600°C, obtained by direct polarization; 242 transients were recorded with a recycle delay of 240 s.

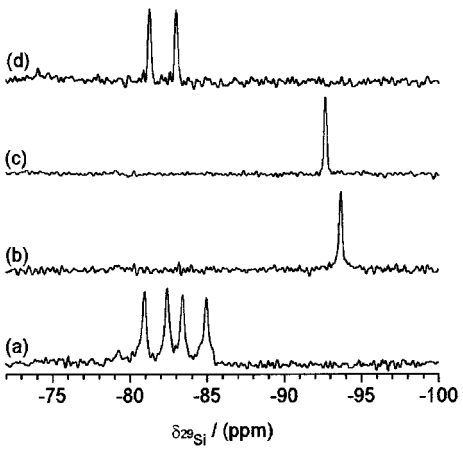

FIG. 2. Direct polarization ^{29}Si spectra of (a) α-$Y_2Si_2O_7$ (b) β-$Y_2Si_2O_7$ (c) γ-$Y_2Si_2O_7$ (d) δ-$Y_2Si_2O_7$; 72, 1, 4, and 44 transients were recorded with 300, –, 600, and 300 s as recycle delays, respectively.

and $[SiO_4]^{4-}$ $[Si_3O_{10}]^{8-}$). This fact would explain why preferential crystallization of α-phase was observed after short isothermal treatments (3 min), whatever the temperature. For temperatures higher than 1225°C, the limit of its thermal stability, α is formed in a metastable state, the driving force probably being the higher rate of crystallization of this phase compared to the other form due to the smaller amount of structural reconstruction needed.

The first ^{29}Si MAS NMR spectra of crystalline $Y_2Si_2O_7$ reported in the literature are those of the γ and δ forms (20), the two peaks for δ being hardly resolved. Smith (21) has recorded some relatively broad spectra for α, β, γ, and δ (for δ, the two peaks are still scarcely distinguished and for α one broad peak is observed). In addition, the spectra exhibit substantial spinning sidebands, which Smith attributed to the chemical shift anisotropy. Other measurements of the chemical shifts for β and γ can be found in Refs. (22) and (23). Figure 2 shows resolved ^{29}Si MAS spectra for the α, β, γ, and δ phases. These spectra have been recorded for samples synthesized under the best conditions and containing the minimum amount of secondary phases. For all forms, peaks corresponding to each unique silicon site in the crystal structure (i.e., 4 for α, 2 for δ, and 1 for β and for γ) are observed for the first time. No spurious signals from other phases were observed because the lines from the $Y_2Si_2O_7$ polymorphs are so sharp (and hence so intense) that other signals such as apatite, which have lines between 10 and 15 times broader (24), are considerably less intense and cannot be distinguished from the background, for the small number of accumulated spectra (between 1 and 74). As we did not observe any spinning sidebands in the present work, we think that the sidebands reported by Smith (21) may be the result of paramagnetic impurities in his samples, though it must be said that Smith's spectra were obtained at a slightly higher magnetic field, 8.45 T, than ours but at similar spinning speeds. Such impurities would also explain the broader peaks and the lack of resolution for the α and δ forms observed. The lower chemical shifts for Q^1 silicon environments in the β and γ forms compared with those of α and δ can be correlated with the (Si–O–Si) bond angles, which are larger in β (180°) (1, 6) and γ (172°) than in α (133.2° and 118.2°) and δ (158°) (1, 6). The same correlation may explain the slight difference in chemical shifts between the β and γ forms. The different silicon environments of the α form (Q^0, Q^1, Q^2) give signals nearly at the same chemical shifts and it is difficult to assign the peaks (25), although the spectrum is perfectly resolved. It is tempting to suggest that the extreme high- and low-frequency peaks arise from Q^0 and Q^2 sites, respectively, and that the middle two signals may be assigned to Q^1 silicons, but to prove this is not easy. Static spectra, though in principle giving a distinction (26), are unlikely to be definitive in the present case, even in a two-dimensional experiment, given the proximity of the signals. A detailed evaluation of geometries reported for relevant rare earth disilicates (1, 7) does not give clear correlations with the shifts we observe for the four yttrium compounds, either via Si–O–Si bond angles or with Si–O distances (27). Presumably both are important, but the situation is probably complicated by cation effects. Accurate geometrical information for all four yttrium disilicates would be required for further progress on assignments to be made.

A spectrum of the y form (not shown) has also been recorded, but shows a poor-quality weak signal with a mean shift of approximately -83 ppm. The ^{29}Si chemical shifts and linewidths for α-, β-, γ-, and δ-$Y_2Si_2O_7$ are summarized in Table 3, along with the corresponding literature references.

4. CONCLUSIONS

Differences in the ranges of stability for the various polymorphs of $Y_2Si_2O_7$ have been observed and compared with previously reported work. Different results were obtained depending on the synthesis route and the thermal history of the sample. High-resolution, high-quality ^{29}Si MAS NMR spectra of the α-, β-, γ-, and δ-$Y_2Si_2O_7$ structural forms have been obtained and are consistent with the reported crystallographic data.

The temperature ranges observed here for polymorph stability are slightly different from those reported in the literature (2). Because the sol–gel process uses chemical precursors of great purity, the presence of impurities, with the exception of H^+, could not be invoked to explain this behavior. It is worth noting that above 900°C our samples were almost all isothermally calcined from an amorphous state, and this had never been studied before. For short heat treatment times (3 min) and whatever the temperature, the

TABLE 3

Chemical Shift (δ_{iso}) and FWHH (Full Width Half Height) for the Different Yttrium Disilicates, Measured for ^{29}Si MAS NMR Spectra

		This work		Literature data	
Phase	Treatment	δ_{iso} (ppm)	FWHH (Hz)	Ref. (21) δ_{iso} (ppm)	Ref. (20) δ_{iso} (ppm)
α	SG, 1200°C 24 h I, Q	−80.96	21	−83.4	—
		−82.43	20		
		−83.41	20		
		−84.95	20		
β	SG, 1350°C 24 h I, Q	−93.65	14	−93.6	—
γ	MP, 1400°C 6 h	−92.68	13	−92.8	−92.9
δ	MP, 1700°C 2 h	−81.27	14	−81.2[a]	−81.6[a]
		−83.00	15	−82.9[a]	−83.5[a]
y	SG, 900°C 24 h	−83.0[a]	—		—

[a]Poor signal-to-noise ratio.

main phase observed was, surprisingly, α and not the stable phases expected for the particular temperature used. Actually, for this kind of heat-treatment and precursors, the process can be considered as a crystallization process (amorphous → crystalline) rather than a solid–solid transformation (crystalline phase → other crystalline phase) as previously studied. Moreover, the structural environment of the silicon species in the starting xerogel, which is quite similar to α, seems to promote the preferential crystallization of this phase (even in a metastable state at temperatures higher than 1225°C). Indeed, the system does not seem to crystallize directly to any structural form with the lowest free energy without passing through the α form, for which the kinetics of formation are the fastest compared to the others because of the minimal amount of structural reconstruction required.

REFERENCES

1. J. Felsche, *Structure Bonding* **13,** 100 (1973).
2. J. Ito and H. Johnson, *Amer. Miner.* **5,** 1940 (1968).
3. E. G. Protosenko, *Zap. Vses. Mineral. Obshch.* **91,** 260 (1962).
4. N. G. Batalieva and Y. A. Pyatenko, *Sov. Phys. Crystallogr.* **16,** 786 (1972).
5. K. Liddell and D. P. Thompson, private communication, 1997.
6. Y. I. Smolin and Y. F. Shepelev, *Acta Crystallogr. B* **26,** 484 (1970).
7. A. N. Christensen, R. G. Hazell, and A. W. Hewat, *Acta. Chem. Scand.* **51,** 37 (1997).
8. D. P. Thompson, *in* "Proceedings International Symposium on Tailoring Multiphase and Composite Ceramics" (R. E. Tressler, G. L. Messing, C. G. Pantano, and R. E. Newnham, Eds.), Vol. 20, p. 79. Penn State University, Materials Science Research, 1986.
9. J. Dodsworth and D. P. Thompson, *Special Ceramics* **7,** 51 (1981).
10. M. Mitomo, F. Izumi, S. Horiuchi, and Y. Matsui, *J. Mater. Sci.* **17,** 2359 (1982).
11. D. P. Thompson, *Mater. Res. Soc. Symp. Proc.* (Materials Research Society) **287,** 79 (1993).
12. M. Sebai, Ph. D. Thesis, Université de Limoges, France, 1996.
13. D. Foster, L. Audoin, P. Goursat, W. Young, L. K. L. Falk, H. Lemercier, S. Hampshire, and D. P. Thompson, *in* "Proc. 9th CIMTEC World Ceramics Congress, "Getting into the 2000s, Part A" (P. Vincenzini, Ed.), p. 397. Publ. Techna SRI, 1999.
14. K. Liddell and D. P. Thompson, *J. Mater. Sci.* **32,** 887–892 (1997).
15. J. C. Hulling and G. L. Messing, *J. Am. Ceram. Soc.* **74**(16), 2374 (1991).
16. D. W. Li and J. Thompson, *J. Am. Ceram. Soc.* **74**(3), 574 (1991).
17. J. Parmentier, K. Liddell, D. P. Thompson, H. Lemercier, N. Schneider, S. Hampshire, P. R. Bodart, and R. K. Harris, submitted for publication.
18. K. Liddell and D. P. Thompson, *Br. Ceram. Trans. J.* **85,** 17 (1986).
19. T. R. Dinger, R. S. Rai, and G. Thomas, *J. Am. Ceram. Soc.* **71**(4), 236 (1988).
20. A. R. Grimmer, F. von Lampe, M. Mägi, and E. Lippmaa, *Monat. Chem.* **115,** 561 (1984).
21. M. E. Smith, Ph. D. Thesis, University of Warwick, 1987.
22. R. Dupree, M. H. Lewis, and M. E. Smith, *J. Am. Chem. Soc.* **110,** 1083 (1988).
23. D. Kruppa, R. Dupree, and M. H. Lewis, *Mater. Lett.* **11,** 195 (1991).
24. R. K. Harris, M. J. Leach, and D. P. Thompson, *Materials* **1,** 336 (1989).
25. M. Magi, E. Lipmaa, A. Samoson, G. Engelhardt, A. R. Grimmer, *J. Phys. Chem.* **88,** 1518 (1998).
26. A. R. Grimmer, *in* "Application of NMR Spectroscopy to Cement Science" (P. Colombet and A.-R. Grimmer, Eds.), Chap. II. 7, p. 118. Gordon & Breach, New York, 1994.
27. G. Englehardt and D. Michel, "High Resolution Solid State NMR of Silicates and Zeolites," p. 29. Wiley, New York, 1987.